

AN ANALYSIS OF THE BROADBAND (22–3900 MHz) RADIO SPECTRUM OF HB 3 (G132.7+1.3): THE DETECTION OF THERMAL RADIO EMISSION FROM AN EVOLVED SUPERNOVA REMNANT?

D. UROŠEVIĆ,^{1,2} T. G. PANNUTI,^{3,4} AND D. LEAHY⁵

Received 2006 June 11; accepted 2006 December 13; published 2007 January 10

ABSTRACT

We present an analysis of the broadband radio spectrum (from 22 to 3900 MHz) of the Galactic supernova remnant (SNR) HB 3 (G132.7+1.3). Published observations have revealed that a curvature is present in the radio spectrum of this SNR, indicating that a single synchrotron component appears insufficient to adequately fit the spectrum. We present here a fit to this spectrum using a combination of a synchrotron component and a thermal bremsstrahlung component. We discuss properties of the latter component and estimate the ambient density implied by the presence of this component to be $n \sim 10 \text{ cm}^{-3}$. We have also analyzed X-ray spectra extracted from archived ASCA GIS observations of different regions of HB 3 to obtain independent estimates of the density of the surrounding interstellar medium (ISM). From this analysis, we have derived electron densities of $(0.1\text{--}0.4)f^{-1/2} \text{ cm}^{-3}$ for the ISM for the three different regions of the SNR, where f is the volume filling factor. By comparing these density estimates with the estimate derived from the thermal bremsstrahlung component, we argue that the radio thermal bremsstrahlung emission is emitted from a thin shell enclosing HB 3. The presence of this thermal bremsstrahlung component in the radio spectrum of HB 3 suggests that this SNR is in fact interacting with an adjacent molecular cloud associated with the H II region W3. By extension, we argue that the presence of thermal emission at radio wavelengths may be a useful tool for identifying interactions between SNRs and molecular clouds, and for estimating the ambient density near SNRs using radio continuum data.

Subject headings: ISM: individual (G132.7+1.3, HB 3) — radiation mechanisms: thermal — radio continuum: general — supernova remnants

1. INTRODUCTION

It has been firmly established that the dominant emission mechanism from Galactic supernova remnants (SNRs) at radio frequencies is synchrotron emission. This conclusion has been reached based on the measured spectral index α of the observed radio emission ($S_\nu \sim \nu^{-\alpha}$) from these sources ranges from ≈ 0.3 to 0.7 (Green 2006), and in some cases, the detection of polarized radio emission. Typically, the radio emission from Galactic SNRs can be modeled by a single power law; however, in the cases of some SNRs, observations over a very broad range of radio frequencies reveal a curvature in the spectra of these sources. Two scenarios have been presented in the literature to explain this observed curvature: the first scenario invokes spectral index variations due to different populations of synchrotron-emitting electrons associated with the SNR (e.g., Tian & Leahy 2005), while the second scenario argues for the presence of a thermal bremsstrahlung component in the radio emission from the SNR in addition to the synchrotron component. This thermal bremsstrahlung component is expected to be most prominent for evolved SNRs interacting with molecular clouds (Urošević et al. 2003a, 2003b; Urošević & Pannuti 2005).

To critically evaluate these two proposed scenarios, we present an analysis of the broadband (22–3900 MHz) radio spec-

trum of one Galactic SNR known to feature a curvature in its radio spectrum, HB 3 (G132.7+1.3). This source has been the subject of extensive radio continuum, H I and OH observations (Brown & Hazard 1953; Landecker et al. 1987; Routledge et al. 1991; Koralesky et al. 1998; Tian & Leahy 2005), which have revealed a shell-like radio morphology for this source with an angular diameter of approximately $80'$. The spectral index of this source is $\alpha = 0.4$, and the measured integrated flux density at 1 GHz is 45 Jy (Green 2006); radio observations of this SNR are complicated by confusing thermal emission from the adjacent H II region W3. Thermal emission from an X-ray-emitting plasma located in the interior of HB 3 was discovered by *Einstein* and described by Leahy et al. (1985). This X-ray emission is seen to lie entirely within the radio shell of HB 3 (Leahy et al. 1985); this combination of a radio shell morphology with a center-filled thermal X-ray morphology has led to the classification of HB 3 as a mixed-morphology SNR (Rho & Petre 1998). In this Letter, we separately model the broadband radio spectrum of HB 3 with a thermal bremsstrahlung component combined with a synchrotron component; from this modeling we obtain an estimate of the density of the ambient interstellar medium (ISM) surrounding HB 3. We compare this estimate to ambient density estimates obtained by analyzing extracted X-ray spectra of this SNR; we then discuss a possible interaction between HB 3 and W3.

2. MODELING THERMAL BREMSSTRAHLUNG EMISSION AT RADIO FREQUENCIES FROM HB 3

As described in previous works (Urošević et al. 2003a, 2003b; Urošević & Pannuti 2005), thermal bremsstrahlung emission may become a significant emission process at radio frequencies for evolved SNRs that are expanding into regions of the interstellar medium (ISM) with enhanced densities such as a molecular cloud. The volume emissivity ϵ_ν (in cgs units) of thermal bremsstrahlung emission for an ionized gas cloud

¹ Department of Astronomy, Faculty of Mathematics, University of Belgrade, Belgrade, Serbia and Montenegro; dejanu@matf.bg.ac.yu.

² Institute Isaac Newton of Chile, Yugoslavia Branch, and Universidad Diego Portales, Chile.

³ Space Science Center, Morehead State University, 200A Chandler Place, Morehead, KY 40351; t.pannuti@morehead-st.edu.

⁴ Guest User, Canadian Astronomy Data Center, which is operated by the Dominion Astrophysical Observatory for the National Research Council of Canada's Herzberg Institute for Astrophysics.

⁵ Department of Physics and Astronomy, University of Calgary, Calgary, AB, Canada; Leahy@ucalgary.ca.

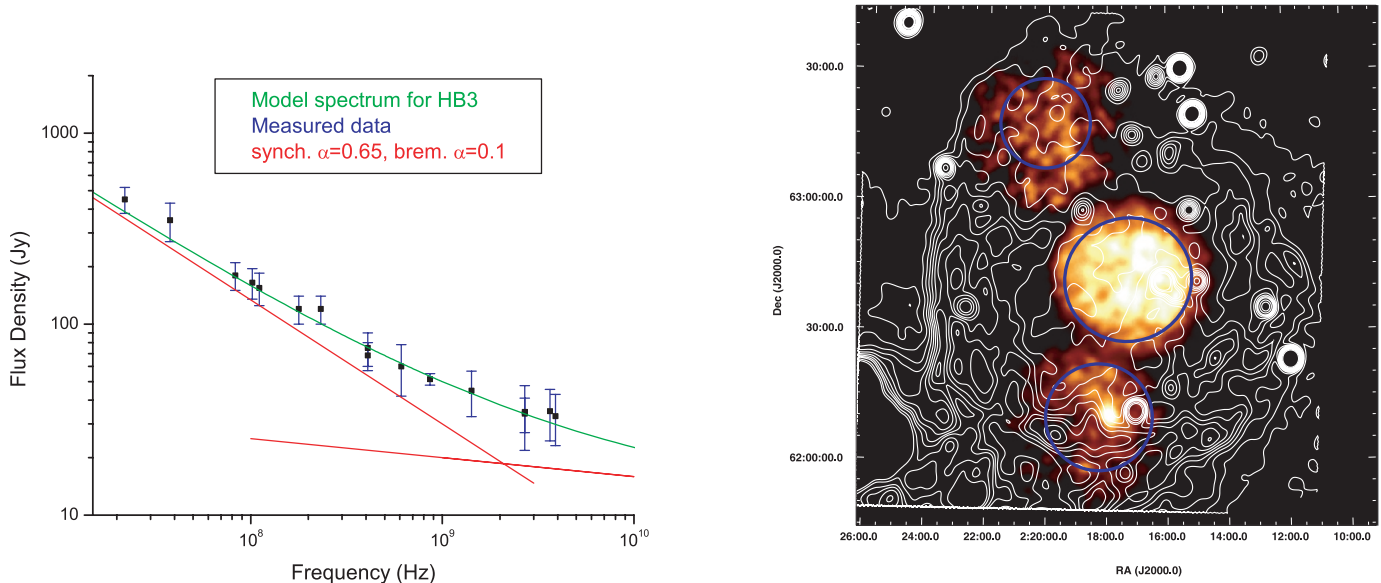


FIG. 1.—*Left*: Broadband radio spectrum of HB 3 based on measured flux densities for this SNR as compiled by Tian & Leahy (2005) as fit with the two-component model (synchrotron and thermal bremsstrahlung). *Right*: ASCA GIS mosaicked image of HB 3; the image has been background subtracted, exposure corrected, and smoothed with a Gaussian of $1'$. The pixel range of the X-ray emission is 0 to 1.43×10^{-4} counts s^{-1} pixel $^{-1}$. Radio emission (408 MHz) has been overlaid in white contours; the contour levels are 60, 65, 70, 75, 80, 85, 90, 95, 100, 110, and 120 mJy beam $^{-1}$. The regions of spectral extraction are marked with blue circles and ellipses.

is proportional to the square of the electron (or ion) volume density n , i.e. (Rohlf & Wilson 1996),

$$\epsilon_{\nu}(\text{ergs s}^{-1} \text{cm}^{-3} \text{Hz}^{-1}) = 7 \times 10^{-38} n^2 T^{-1/2}, \quad (1)$$

where T is the thermodynamic temperature of the ISM. The presence of a significant amount of thermal bremsstrahlung emission will produce a curvature in the observed radio spectrum of the SNR, particularly for frequencies of 1 GHz and greater. Tian & Leahy (2005) showed that spectral flattening exists in the radio spectrum of HB 3 at higher frequencies and argued that this flattening originates from synchrotron emission from different populations of electrons with a range of energy (spectral) indices in low, middle, and high radio frequency domains. For comparison, we have modeled the radio spectrum of HB 3 using a single synchrotron component combined with an additional thermal bremsstrahlung component. For this artificially generated spectrum, we assume that the amount of thermal bremsstrahlung emission is 40%, and the amount of synchrotron emission is 60% of total emission at 1 GHz. In addition, we generated an artificial spectrum using an approximately “pure” synchrotron component with a spectral index $\alpha = 0.65$. This value for α was obtained by fitting the radio flux density from HB 3 over the low-frequency range 22–178 MHz (we expect that the thermal component should account for 10%–25% of the observed radio flux density over this frequency range) and a thermal component with a spectral index $\alpha = 0.1$. Based on these parameters, we calculated the frequency spectrum over 10^7 – 10^{11} Hz. In Figure 1 (*left*) we present both the resulting spectrum (plotted with a thick line) and the measured flux densities for HB 3 over this frequency range compiled by Tian & Leahy (2005, and references therein). From inspection of this figure it is clear that the inclusion of a thermal component produces a noticeable bend in the radio spectrum, which fits the observed radio spectrum well. We therefore argue that the total radio spectrum of HB 3 is

successfully modeled as the sum of synchrotron and thermal bremsstrahlung components.

Based on the properties of the thermal component used to fit the radio spectrum of HB 3, we can estimate the ambient density of the ISM into which the SNR is expanding as follows. Using values obtained from radio observations (such as flux density S_{ν} , diameter D , and thickness of SNR shell s) assuming a distance to HB 3 of 2 kpc (Routledge et al. 1991) and an electron temperature $T = 10^4$ K, we use the relation given in equation (1) to calculate the volume emissivity. Specifically, Tian & Leahy (2005) reported $S_{1 \text{ GHz}} = 50$ Jy, $D = 70$ pc. Using $s = 0.05D$ as a reasonable estimate for shell thickness of evolved SNRs, we obtain $\epsilon_{\nu} = 1.67 \times 10^{-37}$ ergs s^{-1} cm^{-3} Hz^{-1} . From equation (1) and assuming that the thermal component produces 40% of the total radio emission from HB 3 at 1 GHz, we estimate that the density of the ISM into which HB 3 is expanding is $\approx 10 \text{ cm}^{-3}$.

3. X-RAY EMISSION FROM HB 3

Because the X-ray emission from HB 3 extends over such a large angular extent on the sky, pointed observations were conducted with the *Advanced Satellite for Cosmology and Astrophysics* (ASCA) of three different regions (hereafter referred to as the northern region, the central region, and the southern region) to ensure that virtually all of the X-ray emission from HB 3 was sampled. The bulk of this emission originates from the central region where a prominent ring (approximately $35'$ in diameter) of emission is seen (Leahy et al. 1985). The significant variation in the X-ray brightness of HB 3 from one portion of the SNR to another clearly indicates that a wide range exists in the density of the X-ray emitting gas. To help quantify the range of this variation, we analyzed extracted spectra of the emission from each of the three sampled regions as sampled by the two Gas Imaging Spectrometers (GIS), denoted as GIS2 and GIS3, which were aboard ASCA and collected

TABLE 1
SUMMARY OF ASCA GIS OBSERVATIONS OF HB 3 (G132.7+1.3)

Sequence Number	Observation Date	Sampled Region of HB 3	R.A. (J2000.0)	Decl. (J2000.0)	GIS2 Effective Exposure Time (s)	GIS2 Count Rate (counts s ⁻¹)	GIS3 Effective Time Exposure (s)	GIS3 Count Rate (counts s ⁻¹)
54009000	1996 Aug 27	South	02 18 43 7	+62 08 29	13406	0.2591	13404	0.2660
54009010	1996 Aug 28	Center	02 17 07 5	+62 42 55	29720	0.3806	31633	0.4075
54009020	1996 Aug 29	North	02 19 53 9	+63 16 53	9261	0.2399	9260	0.2585

NOTE.—The units of right ascension are hours, minutes, and seconds, and the units of declination are degrees, arcminutes, and arcseconds. Count rates are for the energy range 0.7–10.0 keV.

data during these observations. Details of the GIS observations of HB 3 are provided in Table 1.

The data reduction for the two observations was conducted using the XSELECT program (version 2.2), which is available from the High Energy Astrophysics Science Archive Research Center (HEASARC).⁶ We extracted both GIS2 and GIS3 spectra using the following extraction regions: for the northern region, we used a circular region with a radius of $\sim 10.3'$ (centered at R.A. 02^h 20^m 06^s, decl. +63° 17' 44"[J2000.0]); for the central region, we used an elliptical region with radii 14.7' \times 14.2' (centered at R.A. 02^h 17^m 17^s, decl. +62° 41' 49"[J2000.0]); and finally for the southern region we used a circular region with a radius of $\sim 12.3'$ (centered at R.A. 02^h 18^m 15.3^s, decl. +62° 10' 05"[J2000.0]). The spectra were extracted in the format of pulse-height amplitude (PHA) files as well as images and event files. High bit-rate and medium bit-rate telemetry data were used, and the standard REV2 screening criteria were applied. For the analysis of the GIS2 and GIS3 spectra, we used the standard response matrix files (RMFs) and the corresponding ancillary response files (ARFs) were prepared using the program ASCAARF (version 3.10) from the FTOOLS software package⁷ (Blackburn 1995). Background spectra and images for both GIS2 and GIS3 were prepared using the FTOOL MKGISBGD (version 1.6). In Figure 1 (*right*), we present the total band (0.7–10.0 keV) mosaicked ASCA GIS2+GIS3 image of X-ray emission from HB 3 with radio (1420 MHz) contours overlaid.

To obtain an independent estimate of the ambient density of the ISM surrounding HB 3, we performed spectral fitting on the extracted ASCA GIS spectra for the three different regions of this SNR. For each of the three regions, we simultaneously fit the extracted GIS2 and GIS3 spectra with a collisional plasma model component with solar elemental abundances known as APEC⁸ (Smith et al. 2001) combined with the PHABS component to model interstellar extinction. Using this combination of components, we were able to derive statistically acceptable fits ($\chi_r^2 \sim 1.2$ or less) for the extracted spectra of the northern and southern regions, with column densities ranging from $N_H \approx 0.2\text{--}0.6 \times 10^{22} \text{ cm}^{-2}$ and temperatures $kT \approx 0.4\text{--}0.6 \text{ keV}$. A statistically acceptable fit to the extracted GIS spectra of the central region could not be obtained with this combination of components. Prominent emission lines associated with magnesium and silicon were seen in the extracted

spectra, so a collisional plasma model component with variable elemental abundances, VAPEC, was implemented with the abundances of those two elements allowed to vary. A Gaussian component was also added to account for an emission line of unknown origin seen near 1.2 keV. A statistically acceptable fit still was not obtained, so additional attempts to fit the spectra using a second component, either an additional APEC component with a higher temperature or a power-law component, were made. A statistically acceptable fit was at last obtained after the addition of either of these later two components. The column densities and temperatures of the lower temperature thermal components are comparable in the two fits ($N_H \sim 0.4\text{--}0.5 \times 10^{22} \text{ cm}^{-2}$ and $kT \sim 0.2 \text{ keV}$, respectively). The temperature of the higher temperature component is $kT \approx 2.2 \text{ keV}$, while the photon index of the power-law component is $\Gamma \approx 2.6$. We note that Leahy et al. (1985) has already discussed the presence of two thermal components in the X-ray emission from the central region of HB 3 as revealed by *Einstein* observations. We also note that a gradient is seen in the column densities of the three different regions, decreasing in proceeding from south to north: this result is consistent with the presence of denser material seen in projection toward the southern half of HB 3. We summarize the results of these spectral fits in Table 2. A separate analysis of the ASCA data for HB 3 has also been analyzed and discussed by Lazendić & Slane (2006).

Using the value for the emission measure of the soft thermal component as derived in fits to the extracted GIS spectra for all three regions, we calculated the corresponding electron density of the ambient ISM for each region. We set each emission measure equal to $(10^{-14}/4\pi d^2)n_e n_H fV$, where d is the distance to HB 3 (assumed to be 2 kpc), n_e and n_H are the electron and hydrogen densities (with $n_H = 1.2n_e$), f is the volume filling factor, and finally V is the volume (assuming that the depth of the emitting region is equal to its radius). From this relation, we calculate electron densities $n_e \approx 0.4f^{-1/2} \text{ cm}^{-3}$ for the central region and $n_e \approx 0.1f^{-1/2} \text{ cm}^{-3}$ for the northern and southern regions (see Table 2).

4. DISCUSSION

For comparison to Tian & Leahy (2005), their Table 2 summarizes the spectral variations: the spectral indices range from 0 to 0.9, with most values between 0.3 and 0.7. The boxes nearest W3 are 9 and 13; they both contain flatter indices than 0.3, especially box 13. It has been suggested that the variable spectral index may be due to multiple populations of electrons, since the normal case of a single population with steeper index at higher energies does not explain the radio spectrum (e.g., their Fig. 3). We are suggesting here that a more natural explanation is synchrotron emission, which dominates at lower frequencies, and bremsstrahlung emission, which dominates at higher frequencies. This is supported by the high thermal elec-

⁶ HEASARC is a service of the Laboratory for High Energy Astrophysics (LHEA) at the National Aeronautics and Space Administration Goddard Space Flight Center (NASA/GSFC) and the High Energy Astrophysics Division of the Smithsonian Astrophysical Observatory (SAO). For more information on HEASARC, please see <http://heasarc.gsfc.nasa.gov>.

⁷ ASCAARF and all of the other programs mentioned in this section are part of the FTOOLS software package. For more information on this software package, please see <http://heasarc.gsfc.nasa.gov/ftools/>.

⁸ Also see <http://hea-www.haravrd.edu/APEC>.

TABLE 2
SUMMARY OF SPECTRAL FITS TO ASCA GIS SPECTRA OF THE DIFFERENT REGIONS OF HB 3

Parameter	PHABS × APEC	PHABS × (VAPEC+APEC+Gaussian)	PHABS × (VAPEC+Power Law+Gaussian)	PHABS × APEC
Region	South	Center	Center	North
χ^2_ν (χ^2/dof)	1.15 (451.33/394)	1.19 (458.26/386)	1.21 (467.82/386)	1.22 (481.18/394)
N_{H} (10^{22} cm^{-2})	$0.55^{+0.17}_{-0.15}$	$0.44^{+0.11}_{-0.12}$	$0.47^{+0.11}_{-0.27}$	$0.16^{+0.08}_{-0.06}$
kT_{low} (keV)	$0.39^{+0.15}_{-0.09}$	$0.22^{+0.06}_{-0.04}$	$0.21^{+0.11}_{-0.07}$	$0.54^{+0.05}_{-0.10}$
Mg	1.0 (frozen)	$2.4^{+1.1}_{-1.2}$	2.9 (>1.0)	1.0 (frozen)
Si	1.0 (frozen)	$4.2^{+3.0}_{-2.2}$	4.6 (>2.0)	1.0 (frozen)
$\text{EM}_{\text{low}}^a/(4\pi d^2/10^{-14})$ (cm^{-5})	2×10^{-2}	0.17	0.19	3×10^{-3}
n_e (cm^{-3})	$0.14f^{-1/2}$	$0.35f^{-1/2}$	$0.38f^{-1/2}$	$0.08f^{-1/2}$
E_{Gauss} (keV)	1.26	1.22	...
Normalization ^b	4.1×10^{-4}	2.0×10^{-4}	...
kT_{high} (keV)	$2.2^{+3.8}_{-0.2}$
$\text{EM}_{\text{high}}^a/(4\pi d^2/10^{-14})$ (cm^{-5})	1.3×10^{-3}
Γ	$2.6^{+1.8}_{-1.4}$...
Normalization ^c	7.4×10^{-4}	...
Absorbed flux ^d ($\text{ergs cm}^{-2} \text{s}^{-1}$)	4.2×10^{-12}	1.6×10^{-11}	1.6×10^{-11}	3.5×10^{-12}
Unabsorbed flux ^d ($\text{ergs cm}^{-2} \text{s}^{-1}$)	2.4×10^{-11}	6.8×10^{-11}	7.0×10^{-11}	5.9×10^{-12}
Luminosity ^d (ergs s^{-1})	1.1×10^{34}	3.3×10^{34}	3.4×10^{34}	2.8×10^{33}

NOTE.— All quoted errors are 90% confidence intervals.

^a Emission measure ($\int n_e n_{\text{H}} dV$, where d is the distance in cm and n_e and n_{H} are the electron and H densities in cm^{-3}).

^b In units of total photons $\text{cm}^{-2} \text{s}^{-1}$ in the line.

^c In units of photons $\text{keV cm}^{-2} \text{s}^{-1}$ at 1 keV.

^d For the energy range 0.7–10.0 keV. The luminosity estimates are for an assumed distance of 2 kpc to HB 3.

tron densities derived from the X-ray observations. One can still produce spatial variation of observed spectral index caused by the spatial variation of relativistic electrons and magnetic field (for the synchrotron component) and of thermal electrons (for the bremsstrahlung component). Here we present only a single fit to illustrate that the general idea of synchrotron plus bremsstrahlung emission is viable.

By comparing the densities implied by our fit to the broadband radio spectrum with a thermal bremsstrahlung component with the densities implied by our X-ray observations, we argue that the density profile is such that ambient material is gathered in a thin shell on the outer edge of HB 3; in fact, the observed thermal bremsstrahlung emission at radio frequencies is produced from this shell. We also claim that the distribution of this material in a shell indicates that HB 3 is in fact interacting with the adjacent molecular cloud W3. There has been some debate previously in the literature regarding such an interaction. Routledge et al. (1991) described the detection (through CO observations) of the molecular bar feature that is partially surrounded by continuum emission from HB 3, suggesting that HB 3 is indeed interacting with this cloud (and by extension

W3). However, Koralesky et al. (1998) failed to find shock-excited maser emission at the nominal boundary between the H II region and the SNR that could clearly be associated with the shock of HB 3. Our results supports interaction between HB 3 and W3; we also note that the gradient in the column densities inferred by the X-ray observations is consistent with the geometry of the known cloud and further supports such an interaction. In fact, the detection of thermal emission at radio frequencies from Galactic SNRs may be a crucial new tool in determining whether these sources are interacting with adjacent molecular clouds and for estimating the ambient density near SNRs using radio continuum data.

We thank an anonymous referee for valuable comments and N. Duric for helpful discussions. D. U. would like to thank T. Angelov and B. Arbutina for discussion on thermal emission from SNRs at radio frequencies. T. G. P. would like to thank J. Rho for discussions of the properties of mixed-morphology SNRs. This work is part of the Project 146012 supported by the Ministry of Science and Environmental Protection of Serbia.

REFERENCES

- Blackburn, J. K. 1995, in ASP Conf. Ser. 77, *Astronomical Data Analysis Software and Systems IV*, ed. R. A. Shaw, H. E. Payne, & J. J. E. Hayes (San Francisco: ASP), 367
- Brown, R. H., & Hazard, C. 1953, *MNRAS*, 113, 123
- Green, D. A. 2006, *A Catalogue of Galactic Supernova Remnants*, 2006 April Ver. (Cambridge: Astrophysics Group, Cavendish Laboratory, Univ. Cambridge), <http://www.mrao.cam.ac.uk/surveys/snrs/>
- Koralesky, B., et al. 1998, *AJ*, 116, 1323
- Landecker, T. L., et al. 1987, *AJ*, 94, 111
- Lazendić, J., & Slane, P. O. 2006, *ApJ*, 647, 350
- Leahy, D. A., et al. 1985, *ApJ*, 294, 183
- Rho, J., & Petre, R. 1998, *ApJ*, 503, L167
- Rohlfs, K., & Wilson, T. L. 1996, *Tools of Radio Astronomy* (New York: Springer)
- Routledge, D., et al. 1991, *A&A*, 247, 529
- Smith, R. K., et al. 2001, *ApJ*, 556, L91
- Tian, W. W., & Leahy, D. 2005, *A&A*, 436, 187
- Urošević, D., Duric, D., Pannuti, T. 2003a, *Serbian Astron. J.*, 166, 61
- . 2003b, *Serbian Astron. J.*, 166, 67
- Urošević, D., & Pannuti, T. G. 2005, *Astropart. Phys.*, 23, 577